Optics Communications 340 (2015) 50–55

Contents lists available at ScienceDirect

Optics Communications

journal homepage: www.elsevier.com/locate/optcom

A reflective fiber-optic refractive index sensor based on multimode interference in a coreless silica fiber

Xinlei Zhou, Ke Chen, Xuefeng Mao, Wei peng, Qingxu Yu *

School of Physics and Optoelectronic Technology, Dalian University of Technology, Dalian, Liaoning 116023, PR China

ARTICLE INFO

Article history:
Received 20 September 2014
Received in revised form
6 November 2014
Accepted 7 November 2014
Available online 2 December 2014

Keywords:
Optical fiber sensor
Multimode interference (MMI)
Refractive index sensing
Coreless silica fiber
End-reflection structure

ABSTRACT

A reflective fiber-optic refractive index (RI) sensor based on multimode interference (MMI) is presented and investigated in this paper. The sensor is made by splicing a small section of coreless silica fiber (CSF) to the standard single mode fiber (SMF). A wide-angle beam propagation method (WA-BPM) is employed for numerical simulation and design of the proposed RI sensor. Based on the simulation results, a RI sensor with a length of 1.7 cm of CSF is fabricated and experimentally studied. Experimental results show that the characteristic wavelength shift has an approximately linear relationship with the RI of the sample. A sensitivity of 141 nm/RIU (refractive index unit) and a resolution of 2.8×10^{-5} are obtained in the RI range from 1.33 to 1.38. As the RI value is higher than 1.38, the sensitivity of the sensor increase rapidly as the RI increase and a maximum sensitivity of 1561 nm/RIU can be achieved, corresponding to a resolution of 2.6×10^{-6}. The experimental results fit well with the numerical simulation results.

1. Introduction

Fiber-optic refractive index (RI) sensors are promising and attractive in chemical and biotechnological applications for their unique advantages, such as high sensitivity, fast response, compact size, the potential for remote sensing and immunity to electromagnetic interferences [1–11]. There are several ways to implement RI sensing, such as using a long period grating (LPG) [5], a surface plasmon resonance (SPR) scheme [6], a muli-D-shaped optical fiber [7], a Fabry–Perot interferometer (FPI) [8], or a singlemode–multimode–singlemode (SMS) fiber structure [9–11]. The sensor based on the SMS fiber structure, for its additional advantages of simple structure, low cost, easy to fabricate and high repeatability, has attracted more researchers' attention. The basic sensing principle of the SMS fiber structure sensor is multimode interference (MMI) in the multimode fiber section, which can be influenced by external perturbations. The SMS fiber structure sensor has demonstrated its great potential in temperature and strain sensing [12–14]. However, for RI sensing, the cladding of the multimode fiber must be removed (usually etched by HF acid), which complicates the fabrication process and decrease the mechanical strength of the sensor. In addition, the SMS structure fiber sensor is not suitable for sensing in some special applications such as in vivo detection as its input and output fiber are separate, which need extra space for output fiber to lead out.

To overcome these shortcomings existing in the SMS structure fiber sensor, we present a compact fiber optic RI sensor based on the coreless silica fiber (CSF) with an end-reflection structure. The proposed sensor consists of a single mode fiber (SMF), used simultaneously as input and output fiber, and a section of CSF with a gold film coated on its one endface, as schematically shown in Fig. 1. The CSF has a similar outside diameter with the SMF, therefore it can be easily spliced with the SMF by a commercial fusion splicer. The CSF can directly probe surrounding RI change without any other operations such as etching, which facilitates the sensor's fabrication process. Additional, the end-reflection structure is suitable for measuring liquid and has great potential in vivo detection.

2. Principle

As shown in Fig. 1, when the light travels from the SMF to the CSF, different modes can be excited in the CSF. These modes propagate along the CSF with different propagation constants, then reflected back by the gold film and finally couples into the SMF again at the interface between the SMF and the CSF. As both the SMF and the CSF have circular cross sections and step-index distributions, only linear polarization modes (LP_{0m}, m is a positive integer) can be excited and the total electric field profile at a distance of z from the interface can be described as [12,13]

* Corresponding author. Fax: +86 411 84708379.
E-mail address: yuqx@dlut.edu.cn (Q. Yu).

http://dx.doi.org/10.1016/j.optcom.2014.11.030
0030-4018/

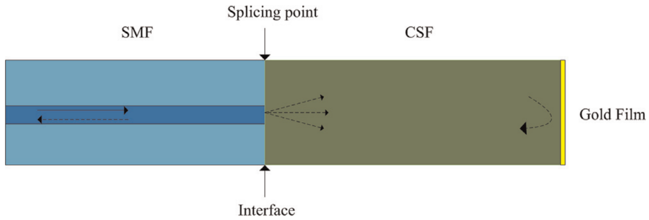

Fig. 1. Schematic diagram of the fiber-optic RI sensor.

$$E(r, z) = \sum_{m=1}^{M} c_m E_m(r)\exp(i\beta_m z) \tag{1}$$

where $E_m(r)$ and β_m are the field profile and longitudinal propagation constant of the mth mode, respectively. c_m is the excitation coefficient from the LP_{01} mode in the SMF to the LP_{0m} mode in the CSF, and can be expressed as

$$c_m = \frac{\int_0^\infty E_s(r)E_m(r)rdr}{\sqrt{\int_0^\infty |E_s(r)|^2 rdr \int_0^\infty |E_m(r)|^2 rdr}} \tag{2}$$

where $E_s(r)$ is the mode field of the LP_{01} mode in the SMF.

The power of the LP_{0m} mode in the CSF is determined by the coupling coefficient η_m, which is

$$\eta_m = c_m^2 \tag{3}$$

A larger coupling coefficient corresponds to a higher power mode. The coupling coefficient for the mode of different orders can vary significantly, as shown in Fig. 2. When these modes couples back into the SMF, MMI will be produced at the interface between the SMF and CSF. Interference between modes with higher coupling coefficients dominates the spectrum response.

Under the weakly guiding condition, the difference of the longitudinal propagation constants between two modes, LP_{0m} and LP_{0n}, can be described as

$$\beta_m - \beta_n = \frac{u_m^2 - u_n^2}{2ka^2 n_c} \tag{4}$$

where $u_m = \pi(m - 1/4)$ and $u_n = \pi(n - 1/4)$ are the roots of the Bessel function of zero order, a is the radius of the CSF, $k = 2\pi/\lambda$ is the wave number and n_c is the refractive index of the CSF. The phase difference between these two modes after propagating a distance z is

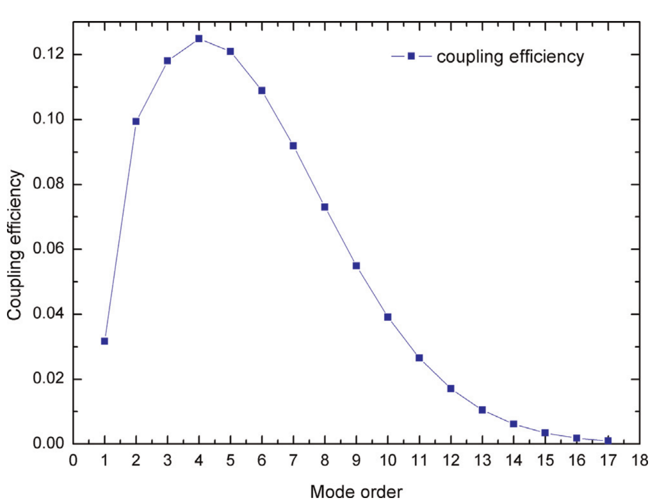

Fig. 2. Calculated coupling coefficients for different order mode with parameters in Table1.

$$\Delta\Phi_{mn} = (\beta_m - \beta_n)z \tag{5}$$

Suppose the length of the CSF is L (corresponding a propagating distance of $2L$), the condition for a constructive or a destructive interference at the SMF–CSF interface is

$$\Delta\Phi_{mn} = (\beta_m - \beta_n)\cdot 2L = \frac{\lambda(u_m^2 - u_n^2)}{4\pi a^2 n_c}\cdot 2L = N\pi \tag{6}$$

where N is an integer. Then we can get the wavelength for a constructive (when N is an even number) or a destructive (when N is an odd number) interference

$$\lambda_c = \frac{4n_c a^2 N}{(m-n)[2(m+n)-1]L} \qquad (m > n) \tag{7}$$

Here, λ_c can be used as the characteristic wavelength for RI sensing. When surrounding RI changes, the boundary condition for the light propagating in the CSF changes, resulting in changes of the coupling coefficient, the longitudinal propagation constant and the mode field profile of each mode. From Eq. (6) we can see that, as the propagation constants changes, the phase condition for the constructive or destructive interference alters and therefore the characteristic wavelength λ_c shifts. The shift of the characteristic wavelength is one to one correspond with the surrounding RI value. Hence, one can get the surrounding RI value by monitoring the characteristic wavelength shift.

3. Numerical simulation

In order to investigate the performance of the sensor and carry out the optimal design of the senor, we conduct some numerical simulations based on the model shown in Fig. 1. Simulations are done using BeamPROP (from Rsoft Inc.), which incorporates computational techniques based on the wide-angle beam propagation method (WA-BPM).

3.1. Field distribution

Simulation is firstly conducted to investigate the field distribution in the CSF. As an example, the parameters selected in this numerical simulation are shown in Table 1.

A Gauss mode with a center wavelength of 1550 nm is used as the incident beam. Fig. 3 shows the simulation results of the propagating field distribution and the normalized propagating power in the CSF. The cross-section of the field distribution at some propagation distances are also presented in Fig. 4(a)–(d). One can see that the light spreads and converges while propagating along the CSF, which is due to the multimode interference. The light power has a minimum (hollow core) at the distance of z=2.92 cm, while it is re-imaged and has a maximum at the distance of z=5.84 cm. In another way, destructive interference and constructive interference occurs at the distance 2.92 cm and 5.84 cm, respectively.

Table 1
Parameters used in simulation.

Items	SMF	CSF
Diameter of core (um)	8.2	0
Refractive index of core	1.4502	0
Diameter of cladding (um)	125	125
Refractive index of cladding	1.445	1.45